

A review of the Application of the Revised Universal Soil Loss Equation for estimation of annual soil loss using conventional methods and GIS

Akshaykumar R Desai¹, V. M. Patel², N. K. Trambadia³

¹PG Scholar, Shantilal Shah Engineering College, Bhavnagar, Gujarat, India

²Professor, Department of Civil Engineering, Shantilal Shah Engineering College, Bhavnagar, Gujarat, India

³Lecturer, Department of Civil Engineering, Sir Bhavsinhji Polytechnic Institute, Bhavnagar, Gujarat, India

Abstract - Soil erosion is currently the most inescapable issue worldwide because of its negative effects on soil fertility, loss of nutrients, loss of biodiversity, deposition of silt materials in the water bodies, and degradation of water quality. There is a vast body of published work on the use of the RUSLE model, also known as the Revised Universal Soil Loss Equation, in conjunction with GIS technology to forecast the hazards of soil loss and erosion in various regions is available. In this paper, we tried an assessment of the RUSLE model's applicability for the estimation of soil loss globally. The Scopus and Google Scholar databases as well as numerous papers about this subject were located. According to the review, RUSLE is the most popular model for estimating soil erosion. It takes into account factors like rainfall erosivity, soil erodibility, slope length and gradient, cover management, and support management practice. These factors depend primarily on climatic conditions, soil classification and properties, slope, land use/land cover, and crop state. Depending on the variability, researchers have developed a set of different empirical equations for these factors of RUSLE. In many parts of the world, this equation can be used to map soil loss. The validation of soil loss using locally accessible data, uniformity in units of different RUSLE variables to avoid mistakes, and estimation of soil loss at monthly temporal data are some of the main future goals for its improvement.

Key Words: RUSLE, soil erosion, GIS, rainfall erosivity, soil erodibility, slope length and steepness, land use - land cover, conservation practice factor

1. INTRODUCTION

The top soil layer is exposed as a result of erosion of the soil. It contributes to soil degradation. Natural physical forces like water, wind, snow, and glaciers produce erosion. When natural forces exert more power than the surface they are acting on can resist, this process takes place. Simply put, soil erosion is the separation of soil particles from their parent material as a result of physical forces. Natural geomorphic processes such as soil erosion and deposition shape landforms and provide fresh parent material for the formation of soil profiles. Accelerated erosion is a situation in which the rate of erosion greatly exceeds the rate that would be expected in the absence of human land usage. These processes create difficulties for soil conservation. The

majority of soil from farmlands is washed away about 10–40 times faster than it is being replaced, according to [1], which cited examples of the United States losing soil at a rate of 10–40 times faster than the average replacement rate and China and India losing soil at a rate of 30–40 times faster. Around 85% of the world's land has been degraded due to soil erosion, the majority of which has happened after the conclusion of World War II and has resulted in a 17% decline in crop output. [2] The sensitivity of the soil to erosion, the characteristics of the land cover, and management practises all have an impact on soil erosion. [3]–[5].

Soil erosion models aid in land management by highlighting the areas vulnerable to soil erosion in the baseline scenario, prospective rates of erosion, and potential causes of soil erosion. They range from conceptual and empirical models that are rather simple to more complex physics-based models [6]. Examples of these include the USLE and GIS-based USLE, WEPP, AGNPS, LISEM, and EUROSEM models. The complexity, inputs, and requirements, the processes they reflect and how they are represented, the range of intended usage, and the types of information they provide as output, however, varies significantly amongst different models [6], [7]. Detailed examinations of soil erosion models of varying complexity have been conducted, however they mainly focus on the input requirements and applications. [3], [6].

The average annual rate of soil erosion (measured in tonnes per unit area) for a particular agricultural system, management strategy, soil type, rainfall pattern, and topographical combination is determined using the empirical USLE model. Its development at the plot scale was initially focused on the agricultural plots of the United States of America [8]. The USLE predicts the long-term average and yearly rate of erosion on a field slope based on rainfall patterns, soil types, topographies, crop systems, and management methods [9]. An upgraded version of USLE (RUSLE) was released, and it included updated rainfall erosivity maps and an improved algorithm for computing the various USLE variables [10]. RUSLE altered the model's incorporation of topographic influence, adding additional variables to denote soil conservation methods, and increased fluctuations in soil erodibility caused by freeze-thaw and soil moisture. He also offered a technique for calculating management and cover parameters [11]. To handle more

complex field settings, the RUSLE2 framework is an updated database of factors and a computer interface [12]. By utilising runoff and peak flow rate to estimate event-based soil loss, the MUSLE is an extension that allows for work at finer temporal resolution [13]. These models are used all around the world because of their apparent simplicity and low data requirements.

Brief discussions of the RUSLE as an empirical model, whose components are frequently included into more complicated conceptual or physics-based soil erosion models, have been reported in extensive reviews of soil erosion modelling and varieties of soil erosion models [3, [6], [14]. Because competing models, such the WEPP, are difficult for most users to use, RUSLE is still often used. Additionally, other researchers discovered a successful technique for figuring out the scope and spatial distribution of erosion by merging remote sensing and GIS methods with soil erosion models like RUSLE. GIS is an effective tool for combining various datasets and assessing dynamic systems, such soil erosion.

The objective is to review the current literature on erosion assessment, which will cover 1) the traditional application of the RUSLE model to assess erosion and 2) the application of GIS and remote sensing methods to forecast and estimate the amount and geographical distribution of erosion at catchment or regional sizes using RUSLE.

2. Conventional Methods for estimation of soil loss using RUSLE

According to the history of soil erosion, there are three key risk factors: rainfall and runoff, the properties of the soil, and plant cover that retains soil. According to [15], Zingg developed the initial equation for quantifying field soil loss in 1940. The effects of slope length and slope steepness on erosion were mathematically described. [16] adds additional cropping systems and support techniques to the equation. According to [10], Browning and colleagues (1947) modified the Smith equation by including soil erodibility and management factors and created extensive tables of the relative factor values for various soil types, crop rotations, and slope lengths. The method focused on assessing slope-length limits for different cropping systems on certain soils, as well as slope steepness with or without terracing, contouring, or strip-cropping.

[15] provided a method for calculating soil losses from clay pan soil areas. There were percentages of soil loss for contour farming, strip farming, and terracing on varied slopes. The suggested slope length upper and lower limitations were specified for contour farming. The equation is also only partially useful because it does not explain what happens to silt once it is eroded. The USLE model is unable to anticipate the path that eroded materials and sediments take as they move from hill slope sites to

water bodies. The design of strategies to control pollution associated with erosion runoff and on agricultural land requires knowledge of what happens in individual rainstorms, rarely on a minute-by-minute basis, in order to predict the size and timing of peak discharges of water and sediment from hill slopes to rivers. The USLE is unable to provide this because it only anticipates mean annual soil loss. The USLE was enhanced in order to highlight the need for an alternative strategy.

3. Methods for the RUSLE model using GIS techniques

RUSLE has been used in a variety of situations, including as large-scale watersheds, tropical watersheds, watersheds where agriculture is the main industry, areas with distinct wet and dry seasons, and areas with dynamic changes in land cover patterns, agricultural cropland, and development. Three essential databases make up the RUSLE model: 1) the meteorological and survey database, which contains the monthly temperature, precipitation, and contour data required to calculate the slope length, steepness factor, and erosivity factor (LS). 2) The crop database contains the data required to calculate the surface cover factor (C). 3) The soil data includes information on soil characterization and soil survey, which can be used to calculate the soil erodibility factor (K).

The use of GIS technology in conjunction with erosion models like the RUSLE has reportedly increased the effectiveness of estimating the spatial distribution and magnitude of erosion risk with reasonable costs and better accuracy, according to a number of researchers whose findings have been published in the literature. [17]–[24].

The RUSLE model calculates the average annual soil erosion loss by accounting for the five variables given in equation 1 [10]. The RUSLE is often implemented by estimating each of the model's factors, which is based on a large body of research. In order to anticipate these variables, previous researchers have developed a number of techniques, including the use of climatic data, soil and geological maps, remotely sensed satellite images, empirical formulas, and digital elevation models (DEM) produced from various sources.

The RUSLE is defined as:

$$A = R \times K \times L \times S \times C \times P$$

Where,

A - Potential long-term average annual soil loss in t

ha-1 yr-1

R - Rainfall erosivity factor in MJ mm ha-1 h-1 yr-1

- K - Soil erodibility factor, Mg h MJ⁻¹ mm⁻¹
- LS - Slope length in m – slope gradient factor in %
- C – Cover management factor
- P - Support practice factor

3.1 Rainfall Erosivity Factor (R)

The rainfall erosivity factor (R) assesses the kinetic energy impact of precipitation and forecasts the amount and rate of runoff that is directly related to that precipitation event. The R factor, which is considered by many experts to be the most important element in RUSLE's assessment of erosion, has a high correlation with soil loss at numerous regional and worldwide rainfall site stations. [8], [11], [25]. Researchers often employ a variety of calculations based on local characteristics and historical rainfall data to calculate the erosion factor. Estimating the R factor might be challenging when there aren't enough data or climate stations. [25] ran across a similar dearth of climate information when assessing the risk of erosion in a particular watershed in Mexico. They used much improved technologies to generate rainfall data. Utilizing techniques like kriging and inverse distance from the remote stations, they interpolated rainfall using remote rainfall stations as a source. Depending on the classification of a research area's climate, [26] published various R-factor formulae.

The equation created by [28] for the Siruvani River watershed in the Attapady Valley of Kerala was applied in India by [27].

$$R = \sum_{i=1}^{12} 1.735 X 10^{(1.5 \log_{10}(\frac{P_i}{p}) - 0.08188)} \quad (1)$$

Where Pi is monthly rainfall (mm), R is rainfall erosivity factor (MJ mm ha⁻¹ h⁻¹ year⁻¹), and P is yearly rainfall (mm).

[29] used it for the Nethravathi Basin in the Middle Western Ghats in India; [30] used it for the Kuttiyadi river basin in Northern Kerala; and [31] used it for the Kali river basin in Karnataka. This equation shows the concept of weighted average precipitation and can be used in a variety of meteorological conditions.

[32] Malaysia adopted the following equation created by Kassam (1992) for his investigation of the Pahang river basin:

$$R = 117.6 * (1.00105^A) \quad (2)$$

Where A = Annual Average rainfall in mm

Tropical climate zones circle the equatorial region. All year long, it pours heavily on a regular basis. The R factor developed by [34] was used by [33] because of the area's humid climate and strong rainfall effects.

$$R = \frac{1}{N} \sum_{i=1}^N (\sum_{m=1}^{12} (7.05 \text{rain}_{10} - 88.92 \text{days}_{10})^m, i) \quad (3)$$

Rain₁₀ represents monthly precipitation only when rainfall C equals 10 mm; otherwise, rain₁₀ is set to zero, where N is the number of years of observations. The number of days in a month where rainfall amount C is 10 mm is day 10. With such a large monthly rainfall, the aforementioned equation generates a high amount of rainfall erosion potential (i.e. rain₁₀). It also demonstrates that, for a given quantity of rainfall, if the number of rainy days is reduced (i.e., to Days 10), the severity of the rainfall and the likelihood of erosion will rise as expected.

A tropical wet and dry climate with reduced rainfall predominates between 5 and 20 latitudes. In this kind of climate zone, rain typically only falls during one season, leaving the other seasons without rain. There is a significant discrepancy in R factor computation in this less humid climate region because of the lack of rainfall.

[35] Used a model that was based on the easily accessible information on that region's annual average rainfall. The equation is written as follows:

$$R = -8.12 + (0.562 * P) \quad (4)$$

Where P is the information on the available yearly average rainfall and R is the rainfall erosivity factor.

The following was created by [36] as another R factor model:

$$R = 79 + 0.363A \quad (5)$$

Where "A" stands for the average annual precipitation in mm and "R" stands for the rainfall erosivity factor.

In semi-arid climate zones, precipitation is insufficient to cover potential evapotranspiration. The numerous varieties of semi-arid climates are determined by temperature variation, which represents the emergence of different forms of ecology.

[37] Created an R factor model specifically for China's dry and semi-arid climate zones:

$$R = (0.1281 \times I_{30B} \times P_f) - (0.1575 \times I_{30B}) \quad (6)$$

Where I_{30B} is a storm's maximum 30-min intensity (mm/h), R is the mean annual rainfall erosivity factor (MJ mm ha⁻¹ h⁻¹ year⁻¹), and P_f is yearly rainfall (mm). The paucity of rainfall in this zone is indicated by Factor I_{30B} .

In the Kianjuki catchment, Embu, Central Kenya, [2] adopted the [10] model, which was used in eastern Africa.

$$R = \frac{1}{n} \sum_{j=1}^n \left[\sum_{k=1}^m (E_k I_{30}) \right]_j \tag{7}$$

Where J is an index that indicates the number of years used to generate the mean of rainfall data, K is an index that indicates the number of storms that occurred in a year, n is the number of years used to obtain the rainfall erosivity factor (R), and M is the number of storms that occur in a year. E is the total kinetic energy produced by the rainfall (MJ ha⁻¹), I_{30} is the maximum of 30-min rainfall intensity (mm h⁻¹).

For their investigation in the Lake Wollumboola catchment, south of Sydney and slightly north of Jervis Bayon, on the New South Wales South Coast, Australia, [38] employed the model created by [10].

3.2 Soil Erodibility Factor (K)

Under typical conditions, the soil's resistance to erosion brought on by the impact of raindrops as well as the rate and volume of runoff that comes from those impacts is shown by the soil erodibility factor (K). According to [39], soil erodibility depends on geological and soil traits as structure, texture, intrinsic material, porosity, organic content, etc. High silt percentages lead to exceptionally erodible soils despite the presence of sizable volumes of sand and clay [40].

The amount of organic matter or carbon in the soil, the molecular bonding or structural class the soil belongs to, the particle size, and the rate of permeability are all elements that determine how easily soil erodes, according to [8]. He produced a nomograph and a model equation based on the equation.

$$K = [2.1 \times 10^{-4} M^{1.14} (12 - OM) + 3.25(S - 2) + 2.5(p - 3)] / 759 \tag{8}$$

Where M is the grain size parameter, which is the product of the silt content (%) (Particles between 0.002 and 0.1 mm in diameter) and (100% clay), and OM is the organic content (%) of the soil. The parameters "s" and "p" describe, respectively, the structure and permeability of the soil.

This concept was applied by [41] in Fort Hood, Texas, USA. This model was applied by [42] to the Wangjiaqiao watershed in Zigui, Hubei, China. employed in

the Chinese Miyun watershed [43]. This equation was used by [44] for the Central Spanish Pyrenees. In Santo Domingo County, Central Chile, South America, [45] applied this empirical approach. For the Keiskamma catchment in South Africa, [40] employed [8] modelling technique. Of the Nun River watershed in Dehradun, Uttarakhand, [46] employed this methodology. [47] applied it to Kothagiri Taluk, Nilgiri, in Tamil Nadu's northwest. For their investigation in the region north of Pune, Maharashtra, [48] used the model. It was used to the Jaipanda watershed in Bankura, West Bengal, by [49].

[50] Created a model that took into account the amount of sand, silt, and clay in the soil as well as the degree of saturation.

$$K = -0.03970 + 0.00311A_1 + 0.00043A_2 + 0.00185A_3 + 0.00258A_4 - 0.00823A_5 \tag{9}$$

Where A_3 is the percentage of the soil's base saturation, A_4 is the percentage of silt present (0.002-0.050 mm), and A_5 is the percentage of sand in the soil. Where A_1 is the percent of unstable aggregates 0.250 mm, A_2 is the product of the percent of silt (0.002-0.01 mm) and sand (0.1-2 mm) present in the sample, and (0.1-2 mm). This model was employed by [2] to estimate the K factor in the Kenyan Highlands of Africa.

Using ideas from the [8] nomograph, [51] created a new model:

$$K = [2.1 \times 10^{-4} M^{1.14} (12 - a) + 4.3 \times 10^{-3} (b - 2) + 3.3(c - 3)] \tag{10}$$

K stands for soil erodibility factor (t ha⁻¹ per unit of R), M for particle size parameter (% silt + % very fine sand) x (100 - % clay), 'a' for organic matter content (in %), 'b' for soil structure code, and 'c' for soil permeability class. Of the Pathri Rao sub-watershed in Uttarakhand,

[52] utilised it. For the Upper Subarnarekha River Basin in Jharkhand, [53] adopted this equation. Model [8] [54] modified as follows:

$$K = 2.77(10^{-7})(12 - \alpha)M^{1.14} + 4.28(10^{-3})(\beta - 2) + 3.29(10^{-3})(\gamma - 3) \tag{11}$$

Where $M = \{(\% \text{ silt} + \% \text{ very fine sand}). (100 - \% \text{ clay})\}$, α is organic matter (in %), β is structure code and γ is permeability rating. [31] Used it for the Nethravathi Basin, the middle region of Western Ghats, India.

Academics are currently using existing soil maps and digitising them to create vector coverage maps in areas where government departments provide soil maps in hard copy format. Then, using data from sources like the Agricultural Handbook or the FAO soil classification system, as suggested by [55] or used by [25], the soils are separated into soil classes. Vector maps were transformed into raster maps using ArcGIS technologies.

The methodology for applying the soil erodibility factor and rainfall erosivity factor, which primarily depend on climatic conditions and soil characteristic regression on soil properties, respectively, was found to differ significantly after examining numerous RUSLE applications used all over the world.

3.3 Slope length and Steepness factor (LS)

The influence of local topography on the rate of soil erosion is described by the slope length (L) and steepness (S) components, which combine the impacts of slope length (L) and slope steepness (S) (S). The slope's length increases both the cumulative run-offs and rate. A higher land slope causes runoff to move more quickly, which causes serious erosion.

When evaluating the topographic impact on erosion, many academics typically include both components (Land S) together. Thanks to GIS technologies, a lot of academics are currently creating topography data using the DEM. The DEM is produced using existing or digitalized contours at predetermined intervals. There are many formulas available for computing topography. Several research have utilised the strategy advised by [15] in their analysis.

$$LS = (Flowaccumulation \times \frac{cellsize}{22.13})^4 (\frac{\sin(slope)}{0.0896})^{1.3} \quad (12)$$

A GIS-integrated prototype of the Sediment Assessment Tool for Effective Erosion Control was created by [56] in order to provide an easy GIS interface for assessing soil erosion and sediment production without the requirement for additional input parameter data beyond those for the USLE model (SATEEC). They applied the method suggested by [15] in the prototype SATEEC to compute the topographical factor from the DEM, providing an upper bound of slope length of 122 m.

[57] developed the LS factor, which is a dimensionless factor in which L is defined as the relative slope length (metres), leaving the LS values virtually the same. The basic slope length was set at 22 m and the basic slope gradient was set at 9%. The LS factor appears as follows:

$$LS = (\frac{\lambda}{\psi})^m (0.065 + 0.046s + 0.0065s^2) \quad (13)$$

the value of Ψ is 22.13 for SI units because the (LS) factor is the ratio of soil loss per unit area from a field slope to that from a length of 22.13 metres, where λ is the flow path length (m or feet), which is denoted as $\lambda =$ (flow accumulation X cell size). S stands for the typical slope gradient (%). $m = 0.2$ for $s < 1$, 0.3 for $1 \leq s < 3$, 0.4 for $3 \leq s < 5$, 0.5 for $5 \leq s < 12$ and 0.6 for $s \geq 12\%$.

[57] Changed the aforementioned model by substituting the sine of the slope angle (θ) for the average slope gradient percentage (%).

$$LS = (\frac{\lambda}{\psi})^m (65.41 \sin^2 \theta + 4.56 \sin \theta + 0.065) \quad (14)$$

Where θ is the slope angle. The value of 'm' is 0.5 if the slope is 5% or more, 'm' is 0.4 if the slope is 3.5–4.5%, 'm' is 0.3 if the slope is 1–3%, and 'm' is 0.2 on uniform where the slope is less than 1%.

This equation was used in India by [53] for the Upper Subarnarekha River basin in Jharkhand. [58] used it for the Mirzapur, Uttar Pradesh, India, Khajuri watershed, Barkachha. [59] used this model in the Kallar Watershed, which is located in the northwest of Tamil Nadu, in the Eastern Ghats. It was used by [31] in India's middle western Ghats region, the Netharavthi basin. [60] used this equation for the West Bengal region's Bakreshwar river basin.

3.4 Cover Management factor (C)

Soil loss is significantly influenced by the kind and quantity of plant cover [61]. In essence, vegetation prevents raindrops from impacting the soil by diffusing the kinetic energy of the rain before it reaches the soil's surface. The amount of plant cover, stage of growth, and kind of vegetation all directly affect the cover management factor (C). Before raindrops hit the soil surface, ground cover usually diffuses their erosive strength; as vegetation cover rises, soil erosion declines. Therefore, vegetation cover and crop cover types are crucial in controlling runoff and erosion rates.

Based on water features, agricultural land, sparse vegetation, dense vegetation, barren land, and built-up land, the cover management factor was first developed by [62]. (Table 1).

Table -1: C factor developed by [62]

Class of Land Use & Land Cover	C factor Value
Built-up	0.000
Agricultural Land	0.400
Dense Vegetation	0.004
Sparse Vegetation	0.030
Barren Land	1.000
Water bodies	0.000

The surface cover factor has historically been determined empirically using measurements of numerous variables connected to ground covers gathered in sample plots. The

weighted average soil loss ratios (SLRs), which are derived from a number of sub-factors including previous land use, canopy cover, surface cover, and surface roughness [64], can also be used to compute it.

However, the method that is currently most frequently used to determine the surface cover factor is to classify the land use and cover using satellite data using remote sensing techniques. Lu et al. (2004) employed fraction images from spectral mixture analysis (SMA) of Landsat ETM+ pictures to estimate the surface cover in their study estimating the danger of soil erosion in the Brazilian Amazonian region. The C factor was calculated using the equation below under the assumption that higher levels of vegetation cover result in less soil loss and lower levels of vegetation cover result in more losses. They do, however, issue a warning that given that surface attributes are recorded at the time of image acquisition, there is still a requirement to calibrate obtained results using local (reference) data when developing the C factor;

$$C = \frac{f_{soil}}{1 + f_{gv} + f_{shade} + f_{gv} \times f_{shade}} \quad (15)$$

Where; C = Vegetative cover and Management factor, and f_{gv} , f_{soil} , f_{shade} = values of green vegetation, soil, and shade endmembers. The three fraction values of soil, green vegetation, and shade endmembers. The values of f_{gv} , f_{soil} , f_{shade} parameters range from 0 to 1 and their sum equals 1.

The remote sensing technique that is most frequently used to determine the C factor is the Normalized Difference Vegetation Index (NDVI). This index, which is determined using the equation below for Landsat-ETM, displays how much energy the planet reflects under various surface cover conditions. The NDVI values' two bands range from -1.0 to +1.0. When the measured spectral response of the earth's surface is roughly comparable to both bands, the NDVI measurements will be closer to zero. A large difference between the two bands is what causes NDVI values at the boundaries of the data range [9].

$$NDVI = \frac{LTM_4 - LTM_3}{LTM_4 + LTM_3} \quad (16)$$

Where; NDVI = Normalized Difference Vegetation Index

The reflectance of actively growing vegetation is higher in the infrared portion of the spectrum (Band 4, Landsat TM) than in the visible region (red, Band 3, Landsat TM), which results in a higher NDVI rating. Clouds and water bodies have negative or zero NDVI values, while low vegetative surface cover has values between -0.1 and +0.1 [9].

For their soil erosion prediction study in Greece, [9] used the NDVI approach to determine the C factor. In accordance with [65], equation was utilised to construct the C factor surface based on the NDVI readings.

$$C = e^{-\alpha \left(\frac{NDVI}{\beta - NDVI} \right)} \quad (17)$$

Where; α and β are unitless parameters that determine the shape of the curve relating to NDVI and C factor.

The C factor was mainly estimated on the basis of various land cover types. [66] developed a model that shows the linear link between the C factor and NDVI. Vegetation difference index normalised. The concept of the NDVI was created by [67];

$$C = 1.02 - 1.21 \times NDVI \quad (18)$$

Where, $NDVI = (NIR - RED) / (NIR + RED)$

In India's Jharkhand province, [68] employed it in the Kharkai river basin. The Subarnarekha river basin in Jharkhand, India, was the subject of its application by [69]. In Bankura, West Bengal, India's Jaipanda Watershed, [49] used it.

The C factor does not linearly vary with NDVI, as initially noted by [65]. In actuality, NDVI causes the C factor to decline dramatically. He created a link between NDVI and C factor that decays exponentially;

$$C = e^{(-\alpha(NDVI/\beta - NDVI))} \quad (19)$$

where α , and β are parameters determining the shape of the NDVI - C curve. A α -value of 2 and a β -value of 1 seem to give reasonable results [65] (Fig. 1).

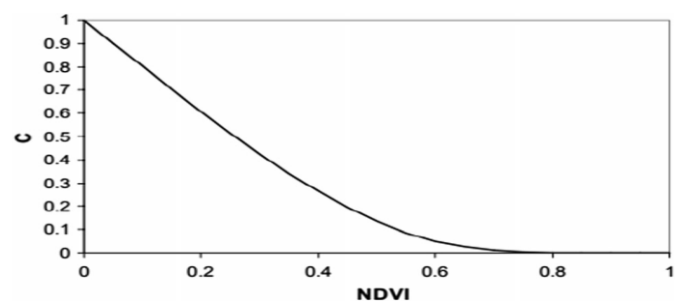


Fig.1 The exponential line used for C calculation from NDVI [65].

This formula was the basis for a lot of Indian researchers' work. For the Siruvani River watershed in the Attapady valley of Kerala, [27] utilised this equation. [70] used this model for the Upper South Koel Basin in Jharkhand. In Kothagiri Taluk, Nilgiri, in the northwest of Tamil Nadu, [47] employed this model. [59] used this model in the

northwest region of Tamil Nadu, the eastern portion of the Western Ghats, and the Kallar watershed. For the Khajuri watershed, Barkachha, Mirzapur, Uttar Pradesh, [58] used it. For the Kuttiyadi river basin in Northern Kerala, [30] used it. [29] applied this equation to the Karnataka region's Kali river basin.

3.5 Conservation practice factor (P)

The conservation or support practise factor (P) demonstrates the effects of taking measures to reduce the rate and volume of runoff, which reduces the rate and volume of soil erosion. The P factor calculates the percentage of soil loss for each support technique, including contour farming, tillage, and slopes both uphill and downhill [57]. [10]. the primary support methods include cross-slope farming, terracing, contour farming, strip cropping, and grassed streams.

The process of creating empirical equations is the one that is most usually used to calculate the conservation factor. [71] used the Wenner technique suggested by [72] to obtain the conservation factor values given by the equation below in China. The slope, which is easily obtained from the provided DEM, is the only quantity required for the equation. In places without conservation and management strategies based on this equation, the P factor value can be employed.

$$P = 0.2 + 0.03 \times S \tag{20}$$

Where; S = slope grade (%)

The P factor estimates the fraction of soil loss for that support technique in the presence of an uphill and downhill slope, contour farming, and tillage [57] and [10]. Contour farming, terracing, strip cropping, cross-slope agriculture, and grassed streams are popular support techniques.

The P values are calculated by dividing the rate and total amount of soil loss resulting from a certain support method by the soil loss occurring from row farming under both uphill and downhill slope conditions, according to [73]. The range of P factor values is 0 to 1. The greatest scores among these values go to areas devoid of any conservation measures (such as grasslands and open spaces), while the lowest ratings go to developed land and plantations that utilise contour cropping.

The conservation practise factor (P) has not yet been defined; the researchers primarily used the P factor's [8] idea in the study region. The P factor chart developed by [8] incorporates all varieties of conservation techniques, and the table is simply adjustable to researchers' own research requirements.

Table -2: P factor for contour ploughing developed by [8]

Land Slope (%)	P Factor Value	Maximum Length (feet)
1-2	0.6	400
3-5	0.5	300
6-8	0.5	200
9-12	0.6	120
13-16	0.7	80
17-20	0.8	60
21-25	0.9	50

However, because there aren't enough conservation practises, they are frequently viewed as a single entity globally.

3.6 Annual Soil Erosion (A)

The five-factor raster map was overlaid with the soil erosion potential and risk map using GIS technologies to determine the overall loss. Usually, the map is broken up into different danger categories, ranging from very low to very high threats. The slope and surface cover both affect risk. The Brazilian Amazonian region was the subject of a study by [74], who found that the danger of soil loss varied from extremely low to low. [9] found a clear correlation between steep slopes and insufficient surface cover in the Crete watershed.

4. CONCLUSIONS & RECOMMENDATIONS

According to the extensive literature study, the RUSLE model has been widely used and has shown to be helpful in estimating soil losses due to erosion in many parts of the world. Despite the fact that RUSLE is a useful model for use at local (small) scales, the integration of RUSLE and GIS techniques has improved the assessment of spatially distributed soil erosion in vast catchment regions. According to the literature, the five fundamental components of the model can be derived from a range of data, such as DEMs, weather data, soil maps, and remote sensing images. Because it provides the necessary capabilities, GIS technology enables the investigation of a larger study area (large-scale watershed) in soil erosion studies.

Future RUSLE model-based GIS research on soil erosion should take into account the following suggestions:

1. Further research into more efficient methods to determine the conservation and management component is required to enhance future studies (P).

2. A crucial step in verifying the accuracy and calibre of the results is to validate the soil erosion loss using locally accessible reference data.
3. To further improve the precision and utility of GIS, additional soil erosion models, such as AGNPS, WEPP, LISEM, and EUROSEM, are also a possibility.
4. Because the origin and calibre of the data are so important to GIS, great care must be given during the pre-processing of the data, which includes converting to numerous formats, georeferencing, data interpolation, and registration.
5. A statistical analysis of the RUSLE parameters is required to ascertain their effect on soil erosion in order to determine which parameter is most crucial.

5. References

- [1] D. Pimentel *et al.*, 'Food Versus Biofuels: Environmental and Economic Costs', *Hum. Ecol.*, vol. 37, no. 1, pp. 1–12, Feb. 2009, doi: 10.1007/s10745-009-9215-8.
- [2] S. D. Angima, D. E. Stott, M. K. O'Neill, C. K. Ong, and G. A. Weesies, 'Soil erosion prediction using RUSLE for central Kenyan highland conditions', *Agric. Ecosyst. Environ.*, vol. 97, no. 1–3, pp. 295–308, Jul. 2003, doi: 10.1016/S0167-8809(03)00011-2.
- [3] H. Aksoy and M. L. Kavvas, 'A review of hillslope and watershed scale erosion and sediment transport models', *CATENA*, vol. 64, no. 2–3, pp. 247–271, Dec. 2005, doi: 10.1016/j.catena.2005.08.008.
- [4] W. David, 'SOIL AND WATER CONSERVATION PLANNING: POLICY ISSUES AND RECOMMENDATIONS', *J. Phillipines Dev.*, vol. 15, no. 1, 1988.
- [5] P. Panagos *et al.*, 'The new assessment of soil loss by water erosion in Europe', *Environ. Sci. Policy*, vol. 54, pp. 438–447, Dec. 2015, doi: 10.1016/j.envsci.2015.08.012.
- [6] W. S. Merritt, R. A. Letcher, and A. J. Jakeman, 'A review of erosion and sediment transport models', *Environ. Model. Softw.*, vol. 18, no. 8–9, pp. 761–799, Oct. 2003, doi: 10.1016/S1364-8152(03)00078-1.
- [7] J. Ismail and S. Ravichandran, 'RUSLE2 Model Application for Soil Erosion Assessment Using Remote Sensing and GIS', *Water Resour. Manag.*, vol. 22, no. 1, pp. 83–102, Jan. 2008, doi: 10.1007/s11269-006-9145-9.
- [8] W. H. Wischmeier and D. D. Smith, *Predicting Rainfall Erosion Losses*. USDA, 1978.
- [9] M. Kouli, P. Soupios, and F. Vallianatos, 'Soil erosion prediction using the Revised Universal Soil Loss Equation (RUSLE) in a GIS framework, Chania, Northwestern Crete, Greece', *Environ. Geol.*, vol. 57, no. 3, pp. 483–497, Apr. 2009, doi: 10.1007/s00254-008-1318-9.
- [10] K. G. Renard and Foster G.R, *Predicting Soil erosion by water: A guide to conservation planning with the Revised Universal soil loss equation (RUSLE)*. USDA, 1997.
- [11] Renard K.G and Freimund J R, 'Using monthly precipitation data to estimate the R-factor in the revised USLE', *J. Hydrol.*, vol. 157, pp. 287–306, 1994.
- [12] Foster G.R, Toy T.E, and Renard K.G, 'Comparison of the USLE, RUSLE1.06c, and RUSLE2 for Application to Highly Disturbed Lands', presented at the First Interagency Conference on Research in Watersheds, Oct. 2003, pp. 154–160.
- [13] S. H. R. Sadeghi, L. Gholami, A. Khaledi Darvishan, and P. Saeidi, 'A review of the application of the MUSLE model worldwide', *Hydrol. Sci. J.*, vol. 59, no. 2, pp. 365–375, Feb. 2014, doi: 10.1080/02626667.2013.866239.
- [14] J. de Vente and J. Poesen, 'Predicting soil erosion and sediment yield at the basin scale: Scale issues and semi-quantitative models', *Earth-Sci. Rev.*, vol. 71, no. 1–2, pp. 95–125, Jun. 2005, doi: 10.1016/j.earscirev.2005.02.002.
- [15] I. D. Moore and G. J. Burch, 'Physical Basis of the Length-slope Factor in the Universal Soil Loss Equation', *Soil Sci. Soc. Am. J.*, vol. 50, no. 5, pp. 1294–1298, Sep. 1986, doi: 10.2136/sssaj1986.03615995005000050042x.
- [16] Smith L.P, 'Agricultural Climate of England and Wales: A Real Averages 1941-70', *Technical Bulletin*, 1976.
- [17] C. Cox and C. Madramootoo, 'Application of geographic information systems in watershed management planning in St. Lucia', *Comput. Electron. Agric.*, vol. 20, no. 3, pp. 229–250, Aug. 1998, doi: 10.1016/S0168-1699(98)00021-0.
- [18] A. M. Dziejowski, A. L. Hales, and E. R. Lapwood, 'Parametrically simple earth models consistent with geophysical data', *Phys. Earth Planet. Inter.*, vol. 10, no. 1, pp. 12–48, May 1975, doi: 10.1016/0031-9201(75)90017-5.
- [19] E. H. Erdogan, G. Erpul, and İ. Bayramin, 'Use of USLE/GIS Methodology for Predicting Soil Loss in a Semiarid Agricultural Watershed', *Environ. Monit. Assess.*, vol. 131, no. 1–3, pp. 153–161, Jun. 2007, doi: 10.1007/s10661-006-9464-6.
- [20] M. Yitayew, S. J. Pokrzywka, and K. G. Renard, 'USING GIS FOR FACILITATING EROSION ESTIMATION', *Appl. Eng. Agric.*, vol. 15, no. 4, pp. 295–301, 1999, doi: 10.13031/2013.5780.
- [21] A. A. Millward and J. E. Mersey, 'Adapting the RUSLE to model soil erosion potential in a mountainous tropical

- watershed', *CATENA*, vol. 38, no. 2, pp. 109–129, Dec. 1999, doi: 10.1016/S0341-8162(99)00067-3.
- [22] H. Mitasova, J. Hofierka, M. Zlocha, and L. R. Iverson, 'Modelling topographic potential for erosion and deposition using GIS', *Int. J. Geogr. Inf. Syst.*, vol. 10, no. 5, pp. 629–641, Jul. 1996, doi: 10.1080/02693799608902101.
- [23] Molnar D.K, 'Estimation of Upland Erosion using GIS', *J. Comput. Geosci.*, vol. 24, no. 2, pp. 183–192, 1997.
- [24] Wilson J.P and Lorang M.S, *Spatial Models of Soil erosion and GIS*. 1999.
- [25] A. A. Millward and J. E. Mersey, 'Adapting the RUSLE to model soil erosion potential in a mountainous tropical watershed', *CATENA*, vol. 38, no. 2, pp. 109–129, Dec. 1999, doi: 10.1016/S0341-8162(99)00067-3.
- [26] V. Naipal, C. Reick, J. Pongratz, and K. Van Oost, 'Improving the global applicability of the RUSLE model – adjustment of the topographical and rainfall erosivity factors', *Geosci. Model Dev.*, vol. 8, no. 9, pp. 2893–2913, Sep. 2015, doi: 10.5194/gmd-8-2893-2015.
- [27] V. Prasannakumar, R. Shiny, N. Geetha, and H. Vijith, 'Spatial prediction of soil erosion risk by remote sensing, GIS and RUSLE approach: a case study of Siruvani river watershed in Attapady valley, Kerala, India', *Environ. Earth Sci.*, vol. 64, no. 4, pp. 965–972, Oct. 2011, doi: 10.1007/s12665-011-0913-3.
- [28] Arnoldus H, Boedt M, and Gabriels D, 'An approximation of the rainfall factor in the Universal Soil Loss Equation', *John Wiley Sons*, pp. 127–132, 1980.
- [29] V. J. Markose and K. S. Jayappa, 'Soil loss estimation and prioritization of sub-watersheds of Kali River basin, Karnataka, India, using RUSLE and GIS', *Environ. Monit. Assess.*, vol. 188, no. 4, p. 225, Apr. 2016, doi: 10.1007/s10661-016-5218-2.
- [30] Baby A and Nair A G, 'Soil Erosion Estimation of Kuttiyadi River Basin Using RUSLE', *Int. Adv. Res. J. Sci. Eng. Technol.*, vol. 3, no. 3, 2016.
- [31] B. P. Ganasri and H. Ramesh, 'Assessment of soil erosion by RUSLE model using remote sensing and GIS - A case study of Nethravathi Basin', *Geosci. Front.*, vol. 7, no. 6, pp. 953–961, Nov. 2016, doi: 10.1016/j.gsf.2015.10.007.
- [32] Agele D M, Lihan T K, and Rahim S A, 'RISK ASSESSMENT OF SOIL EROSION DOWNSTREAM OF THE PAHANG RIVER BASIN WITH RUSLE MODEL', 2013, vol. 19, pp. 571–580.
- [33] R. Ranzi, T. H. Le, and M. C. Rulli, 'A RUSLE approach to model suspended sediment load in the Lo river (Vietnam): Effects of reservoirs and land use changes', *J. Hydrol.*, vol. 422–423, pp. 17–29, Feb. 2012, doi: 10.1016/j.jhydrol.2011.12.009.
- [34] N. de Santos Loureiro and M. de Azevedo Coutinho, 'A new procedure to estimate the RUSLE EI30 index, based on monthly rainfall data and applied to the Algarve region, Portugal', *J. Hydrol.*, vol. 250, no. 1–4, pp. 12–18, Sep. 2001, doi: 10.1016/S0022-1694(01)00387-0.
- [35] Hurni H, *Soil conservation manual for Ethiopia*. 1985.
- [36] Singh G, Chandra S., and Babu R., 'Soil Loss and Prediction Research in India', *entral Soil and Water Conservation Research Training Institute, Dehradun*, 1981.
- [37] Bu. Z, 'The progress of quantitative remote sensing method for annual soil losses and its application in Taihu-Lake Watersheds', *Acta Pedol Sin.*, no. 40, pp. 1–9, 2003.
- [38] A. D. Simms, C. D. Woodroffe, and B. G. Jones, 'Application of RUSLE for erosion management in a coastal catchment, southern NSW', 2003.
- [39] Schwab G.O, Fangmeier D.D, and Elliot W J, *Soil and Water Conservation Engineering*, 4th ed. John Wiley & Sons, Inc., 1993.
- [40] P. Mhangara, V. Kakembo, and K. J. Lim, 'Soil erosion risk assessment of the Keiskamma catchment, South Africa using GIS and remote sensing', *Environ. Earth Sci.*, vol. 65, no. 7, pp. 2087–2102, Apr. 2012, doi: 10.1007/s12665-011-1190-x.
- [41] P. Parysow, G. Wang, G. Gertner, and A. B. Anderson, 'Spatial uncertainty analysis for mapping soil erodibility based on joint sequential simulation', *CATENA*, vol. 53, no. 1, pp. 65–78, Aug. 2003, doi: 10.1016/S0341-8162(02)00198-4.
- [42] Z. H. Shi, C. F. Cai, S. W. Ding, T. W. Wang, and T. L. Chow, 'Soil conservation planning at the small watershed level using RUSLE with GIS: a case study in the Three Gorge Area of China', *CATENA*, vol. 55, no. 1, pp. 33–48, Jan. 2004, doi: 10.1016/S0341-8162(03)00088-2.
- [43] T. Chen, R. Niu, P. Li, L. Zhang, and B. Du, 'Regional soil erosion risk mapping using RUSLE, GIS, and remote sensing: a case study in Miyun Watershed, North China', *Environ. Earth Sci.*, vol. 63, no. 3, pp. 533–541, Jun. 2011, doi: 10.1007/s12665-010-0715-z.
- [44] M. Lopez-Vicente, A. Navas, and J. Machín, 'Identifying erosive periods by using RUSLE factors in mountain fields of the Central Spanish Pyrenees', preprint, Jul. 2007. doi: 10.5194/hessd-4-2111-2007.
- [45] C. A. Bonilla, J. L. Reyes, and A. Magri, 'Water Erosion Prediction Using the Revised Universal Soil Loss Equation (RUSLE) in a GIS Framework, Central Chile', *Chil. J. Agric. Res.*,

vol. 70, no. 1, Mar. 2010, doi: 10.4067/S0718-58392010000100017.

[46] Naqvi H R, Devi L. M, and Siddiqui M. A, 'Soil loss prediction and prioritization based on revised universal soil loss estimation (RUSLE) model using geospatial technique', *Int. J. Environ. Prot.*, vol. 2, no. 3, pp. 39–43, 2012.

[47] Kartic M, Annadurai R, and Ravichandran P T, 'Assessment of Soil Erosion Susceptibility in Kothagiri Taluk Using Revised Universal Soil Loss Equation (RUSLE) and Geo-Spatial Technology', vol. 4, no. 10, 2014.

[48] V. Joshi, N. Susware, and D. Sinha, 'Estimating soil loss from a watershed in Western Deccan, India, using Revised Universal Soil Loss Equation', *Landsc. Environ.*, vol. 10, no. 1, pp. 13–25, Apr. 2016, doi: 10.21120/LE/10/1/2.

[49] S. C. Pal and M. Shit, 'Application of RUSLE model for soil loss estimation of Jaipanda watershed, West Bengal', *Spat. Inf. Res.*, vol. 25, no. 3, pp. 399–409, Jun. 2017, doi: 10.1007/s41324-017-0107-5.

[50] El-swaify S and Dangler E, 'Erodibilities of selected tropical soils in relation to structural and hydrologic parameters. In G. Foster (Ed.)', *Soil Eros. Predict. Control*, pp. 105–114, 1976.

[51] Foster G.R, McCool D.K, Renard K.G, and Moldenhauer W.C, 'Conversion of the universal soil loss equation to SI metric units', *J. Soil Water Conserv.*, vol. 36, no. 6, pp. 355–359, 1981.

[52] S. Kumar and S. P. S. Kushwaha, 'Modelling soil erosion risk based on RUSLE-3D using GIS in a Shivalik sub-watershed', *J. Earth Syst. Sci.*, vol. 122, no. 2, pp. 389–398, Apr. 2013, doi: 10.1007/s12040-013-0276-0.

[53] S. Chatterjee, A. P. Krishna, and A. P. Sharma, 'Geospatial assessment of soil erosion vulnerability at watershed level in some sections of the Upper Subarnarekha river basin, Jharkhand, India', *Environ. Earth Sci.*, vol. 71, no. 1, pp. 357–374, Jan. 2014, doi: 10.1007/s12665-013-2439-3.

[54] Rosewell C, *Soilloss—A program to assist in the selection of the management practices to reduce erosion*, 2nd ed. 1993.

[55] A. Shamshad, C. S. Leow, A. Ramlah, W. M. A. Wan Hussin, and S. A. Mohd. Sanusi, 'Applications of AnnAGNPS model for soil loss estimation and nutrient loading for Malaysian conditions', *Int. J. Appl. Earth Obs. Geoinformation*, vol. 10, no. 3, pp. 239–252, Sep. 2008, doi: 10.1016/j.jag.2007.10.006.

[56] K. J. Lim, M. Sagong, B. A. Engel, Z. Tang, J. Choi, and K.-S. Kim, 'GIS-based sediment assessment tool', *CATENA*, vol. 64, no. 1, pp. 61–80, Nov. 2005, doi: 10.1016/j.catena.2005.06.013.

[57] D. D. Smith and W. H. Wischmeier, 'Factors affecting sheet and rill erosion', *Trans. Am. Geophys. Union*, vol. 38, no. 6, p. 889, 1957, doi: 10.1029/TR038i006p00889.

[58] D. Agarwal, K. Tongaria, S. Pathak, A. Ohri, and M. Jha, 'SOIL EROSION MAPPING OF WATERSHED IN MIRZAPUR DISTRICT USING RUSLE MODEL IN GIS ENVIRONMENT', *Int. J. Stud. Res. Technol. Manag.*, vol. 4, no. 3, pp. 56–63, Dec. 2016, doi: 10.18510/ijstrtm.2016.433.

[59] S. Abdul Rahaman, S. Aruchamy, R. Jegankumar, and S. Abdul Ajeez, 'ESTIMATION OF ANNUAL AVERAGE SOIL LOSS, BASED ON RUSLE MODEL IN KALLAR WATERSHED, BHAVANI BASIN, TAMIL NADU, INDIA', *ISPRS Ann. Photogramm. Remote Sens. Spat. Inf. Sci.*, vol. II-2/W2, pp. 207–214, Oct. 2015, doi: 10.5194/isprsannals-II-2-W2-207-2015.

[60] G. K. Gopal, M. Sutapa, and P. Swades, 'Surface Runoff and Soil erosion Dynamics: A Case study on Bakreshwar river basin, eastern India', vol. 3, 2015.

[61] L. Benkobi, M. J. Trlica, and J. L. Smith, 'Evaluation of a Refined Surface Cover Subfactor for Use in RUSLE', *J. Range Manag.*, vol. 47, no. 1, p. 74, Jan. 1994, doi: 10.2307/4002845.

[62] USDA-SCS, 'Hydrology' in *SCS national engineering handbook*. Washington DC: US Department of Agriculture., 1972.

[63] K. Ghosal and S. Das Bhattacharya, 'A Review of RUSLE Model', *J. Indian Soc. Remote Sens.*, vol. 48, no. 4, pp. 689–707, Apr. 2020, doi: 10.1007/s12524-019-01097-0.

[64] Renard K.G, Foster G.R, Weesies G A, and Porter J P, 'Revised Universal Soil loss equation', *J. Soil Water Conserv.*, vol. 46, no. 1, pp. 30–33, 1991.

[65] van der Knijff J M, Jones R J A, and Montanarella L, *Soil Erosion Risk Assessment in Europe*. European soil bureau, 2000.

[66] Morgan R, *Soil Erosion and Conservation*, 2nd ed. U.K, 1995.

[67] McFarlane, D, Delroy, N., and Van, S. V, 'Water erosion of potato land in Western Australia', *Aust. J. Soil Water Conserv.*, vol. 4, no. 1, pp. 33–40, 1991.

[68] G. K. Das and R. Guchait, 'Modeling of Risk of Soil Erosion in Kharkai Watershed using RUSLE and TRMM Data: A Geospatial Approach', vol. 5, no. 10, 2013.

[69] R. K. Samanta, G. S. Bhunia, and P. K. shit, 'Spatial modelling of soil erosion susceptibility mapping in lower basin of Subarnarekha river (India) based on geospatial techniques', *Model. Earth Syst. Environ.*, vol. 2, no. 2, p. 99, Jun. 2016, doi: 10.1007/s40808-016-0170-2.

[70] R. Parveen and U. Kumar, 'Integrated Approach of Universal Soil Loss Equation (USLE) and Geographical Information System (GIS) for Soil Loss Risk Assessment in Upper South Koel Basin, Jharkhand', *J. Geogr. Inf. Syst.*, vol. 04, no. 06, pp. 588–596, 2012, doi: 10.4236/jgis.2012.46061.

[71] G. Fu, S. Chen, and D. K. McCool, 'Modeling the impacts of no-till practice on soil erosion and sediment yield with RUSLE, SEDD, and ArcView GIS', *Soil Tillage Res.*, vol. 85, no. 1–2, pp. 38–49, Jan. 2006, doi: 10.1016/j.still.2004.11.009.

[72] A. Lufafa, M. M. Tenywa, M. Isabirye, M. J. G. Majaliwa, and P. L. Woomer, 'Prediction of soil erosion in a Lake Victoria basin catchment using a GIS-based Universal Soil Loss model', *Agric. Syst.*, vol. 76, no. 3, pp. 883–894, Jun. 2003, doi: 10.1016/S0308-521X(02)00012-4.

[73] I. Z. Gitas, K. Douros, C. Minakou, G. N. Silleos, and C. G. Karydas, 'MULTI-TEMPORAL SOIL EROSION RISK ASSESSMENT IN N. CHALKIDIKI USING A MODIFIED USLE RASTER MODEL', 2009.

[74] D. Lu, G. Li, G. S. Valladares, and M. Batistella, 'Mapping soil erosion risk in Rondônia, Brazilian Amazonia: using RUSLE, remote sensing and GIS', *Land Degrad. Dev.*, vol. 15, no. 5, pp. 499–512, Sep. 2004, doi: 10.1002/ldr.634.

[75] K. G. Renard, 'Using monthly precipitation data to estimate the i^* -factor in'.

[76] I. D. Moore and G. J. Burch, 'Physical Basis of the Length-slope Factor in the Universal Soil Loss Equation', *Soil Sci. Soc. Am. J.*, vol. 50, no. 5, pp. 1294–1298, Sep. 1986, doi: 10.2136/sssaj1986.03615995005000050042x.

[77] †The International HapMap Consortium, 'The International HapMap Project', *Nature*, vol. 426, no. 6968, pp. 789–796, Dec. 2003, doi: 10.1038/nature02168.